Available online at www.sciencedirect.com
ScienceDirect
Mendeleev Commun., 2016, **26**, 549–551
Mendeleev Communications

Synthesis and characterization of passivated iron nanoparticles

Michail I. Alymov,[a] Nikolai M. Rubtsov,*[a] Boris S. Seplyarskii,[a] Victor A. Zelensky[b] and Alexey B. Ankudinov[b]

[a] *Institute of Structural Macrokinetics and Materials Science, Russian Academy of Sciences, 142432 Chernogolovka, Moscow Region, Russian Federation. Fax: +7 495 962 8025; e-mail: nmrubtss@mail.ru*
[b] *A. A. Baikov Institute of Metallurgy and Materials Science, Russian Academy of Sciences, 119991 Moscow, Russian Federation*

DOI: 10.1016/j.mencom.2016.11.031

Nanosized iron powders (20–100 nm) were prepared by the reduction of a 1 mm layer of iron(III) hydroxide in a flow of hydrogen at 400 °C and then passivated in a flow of 0.6% oxygen + Ar for 6–60 min. The passivated iron nanoparticles can be stored without significant oxidation for five months.

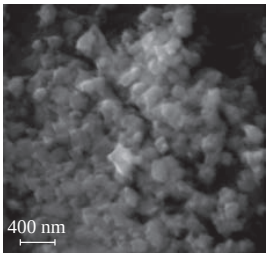

Nanotechnology is the engineering and art of manipulating matter on a nanoscale (1–100 nm).[1–8] In particular, iron nanoparticles are of interest due to their potential application in groundwater treatment and site remediation for the removal of halogenated organic contaminants and heavy metals from the environment.[9–12] In addition, iron nanopowder is effective for the stabilization or destruction of a host of pollutants due to its highly reducing character.[9–18] Thus, relatively cheap iron nanopowder is one of the best reactive materials in permeable reactive barrier technology.[9] The specific surface area of iron nanopowder increases drastically; hence, the surface reactivity of iron nanoparticles becomes about 30 times higher than that of 325 mesh iron powder.[10]

It was found that iron nanopowder can be used to destruct or bind halogenated hydrocarbons,[11] carbon tetrachloride[12] and polychlorinated biphenyls.[13] Moreover, iron nanoparticles are effective for the binding of toxic environmental pollutants like chlorinated organic solvents,[14] organochlorine pesticides,[15] organic dyes,[16] inorganic compounds[17] and metal ions. Field tests have shown the promising properties of iron nanoparticles for *in situ* remediation.[18]

Recently, various synthetic methods have been developed to produce iron nanoparticles and to modify nanoparticle surface properties.[19,20] However, iron nanopowder is unstable under atmospheric conditions and it tends to form the oxides/hydroxides Fe_3O_4, Fe_2O_3 and FeOOH.[21,22] For instance, iron nanoparticles obtained by the reaction

$$2\,FeCl_3 + 6\,NaBH_4 + 18\,H_2O \rightarrow 2\,Fe + 6\,NaCl + 6\,B(OH)_3 + 21\,H_2$$

should be kept under a thin layer of ethanol to avoid oxidation.[22] Therefore, to make possible further processing of nanopowders in ambient air, they should be protected (passivated) with a protective thin oxide or nitride[21] film on the surface of nanoparticles.

The aim of this work was to prepare iron nanoparticles by a chemical metallurgy method and to further passivate them to prevent bulk oxidation. The characterization of the synthesized iron nanopowders was also performed.

The main stages of the production of metal nanopowders include the synthesis, reduction and passivation of metal hydroxides.[23] Iron hydroxide was synthesized by mixing a solid iron salt with an ammonia (threefold excess) solution at pH 9–11:

$$FeCl_3 + 3\,NH_4OH \rightarrow Fe(OH)_3 + 3\,NH_4Cl.$$

After the sedimentation of iron hydroxide, it was washed in a Buchner funnel to pH 7 and dried in air until dusting. A reactor, which was described elsewhere,[24] with a sample of iron hydroxide powder 1 mm thick was heated at 400 °C in a furnace in a flow of hydrogen for 1 h; then, it was cooled to 20 °C in a flow of argon. For the passivation of iron nanopowder in the reactor, 0.6% O_2 was added to a flow of argon at 20 °C. The passivation time varied from 6 to 60 min. Then, the quartz trough with the passivated iron nanopowder was extracted from the reactor.

The passivated iron nanoparticles were characterized using the diffraction determination of the mean size of coherent scattering regions (CSRs), Auger electron spectroscopy, X-ray phase analysis and BET studies.[†]

The CSR size is equal to the mean size of crystallites; generally, it is 10–15% smaller than the size of small particles (grains) identified using electron microscopy, while coherent scattering region corresponds to the inner ordered region of a grain, and it does not include severely distorted boundaries. The CSR size was calculated by an approximation method applicable to structural

[†] The phase structure of the samples was studied on an X-ray Diffray-401 diffractometer (Russia) with a coordinate-sensitive detector using CuKα radiation at room temperature. The Auger electron spectra (AES) were measured on a JEOL JAMP-9500F Auger spectrometer (Japan) with a 3 nm resolution in the secondary emission image (SEI) mode (at 25 kV, 10 Pa). The electronic probe diameter was 8 nm (at 25 kV, 1 Pa), and the accelerating voltage was 0.5–30 kV. The device was equipped with an electrostatic hemispherical analyzer and a multichannel ionic gun (the energy of ions varied from 0.01 to 4 keV). The BET specific surface areas (in a range of 0.01–2000 $m^2\ g^{-1}$) were measured by a NOVA 1200e analyzer (USA) using the low-temperature adsorption of nitrogen.

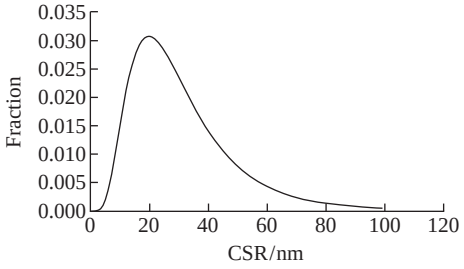

Figure 1 Mean crystallite sizes determined by CSR studies.

components of 20–150 nm in size, which are close to a spherical form and do not have micro tensions; therefore, the size of the objects was underestimated. Calculation was based on the Voigt function for the approximation of X-ray band profiles. Figure 1 shows the results of the determination of the mean size of crystallites in iron nanopowder. The mean size (~30 nm) is the same for the passivation times of 6–60 min, *i.e.* the size does not depend on the passivation time. According to the X-ray phase analysis the nanopowder passivated in 0.6% O_2 + Ar for more than 6 min and stored in a weighing bottle equipped with the ground-in cover within four months contains only metallic iron (Figure 2).

It is known that the mechanism of formation of protective oxide film has diffusive nature;[25–28] therefore, the concentration of oxygen atoms on the surface is markedly greater than that in the volume of a particle. On the other hand, X-ray measurements have shown that the particles after passivation consist of iron (Figure 2). As the X-ray method detects only iron and iron oxides are not detected at all, an oxide layer is quite thin. This is also supported by the main result of the present work implying that the passivated Fe nanoparticles are not oxidized within five months (if the protective film had any defects, or the film was located in any way within the particle, iron would be fully oxidized).

Additional Auger measurements demonstrated agreement with the diffusive passivation mechanism and allowed us to estimate the thickness of the protective oxide film.

Figure 3 depicts the SEI of passivated iron nanoparticles (passivation time, 20 min). The iron particles exist in contact with each other. The AES depth profile analysis for three positions shown in Figure 3 indicates that the passivated particles contain Fe and O atoms along with usually detectable carbon (C) impurity. Note that the values of atomic density are largely qualitative as the probing beam in the position of the analysis can touch the particles lying below as opposed to *e.g.* the analysis of thin films. Thus, the dependences of atomic densities on the depth (etching time) are overstuffed. However, the maximum density of oxygen atoms at a depth of 2 nm is observed in all of these three dependences. This maximum, obviously, correlates with the maximum thickness of passivating oxide film on an iron core.

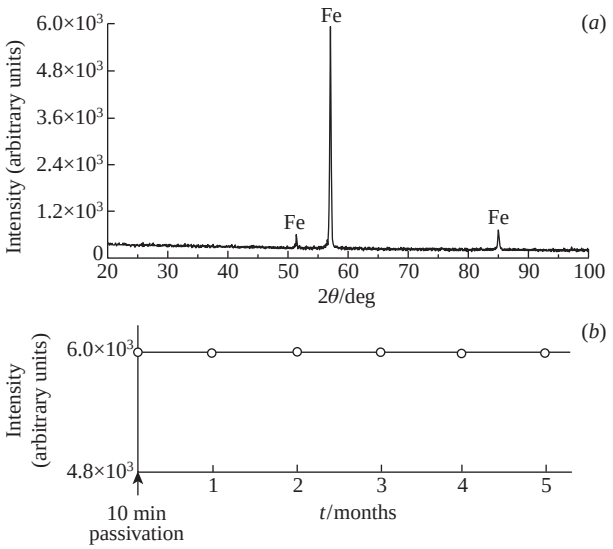

Figure 2 (*a*) X-ray phase analysis of the passivated iron nanopowder (10 min in argon containing 0.6% O_2) stored in a weighing bottle with the ground-in cover within five months. (*b*) Dependence of the intensity of iron in nanopowder after 10 min of passivation on the time of storage of Fe nanopowder in a weighing bottle with the ground-in cover.

Therefore, the mean thickness of passivating oxide film can be estimated at ~2–4 nm.

The BET surface areas were determined as 8.997, 9.077, 9.153, and 9.561 $m^2\ g^{-1}$ for different samples of passivated iron nanoparticles (error, 5–10%). It means that the specific surface does almost not depend on passivation time. Note that the specific surface for a passivation time of 6 min was obtained for a sample of iron hydroxide drained without the use of a Buchner funnel. Thus, the offered method of reduction and passivation is characterized by reproducibility since it gives almost the same value of specific surface. The formula $d = 6/(\rho s)$ if $s = 9.0\ m^2\ g^{-1}$ gives the particle diameter $d = 85$ nm (ρ is the density), *i.e.*, the mean particle diameter lies between an underestimated value (30 nm) and an overestimated one (85 nm).

The BET surface areas reported in the literature are 14.5,[18] 25,[22] 33.5,[29] and 36.5 $m^2\ g^{-1}$.[15] In comparison, a commercial Fe powder (< 10 μm) has a specific surface area of 0.9 $m^2\ g^{-1}$.[15] However, data on the stability of these powders in ambient air were not reported.

Therefore, the chemical metallurgy method along with passivation is effective for the synthesis of 20–100 nm iron nanoparticles stable in ambient air.

The average BET specific surface area of the passivated iron nanoparticles was ~9.2 $m^2\ g^{-1}$ regardless of the passivation time.

This work was supported by the Russian Science Foundation (project no. 16-13-00013).

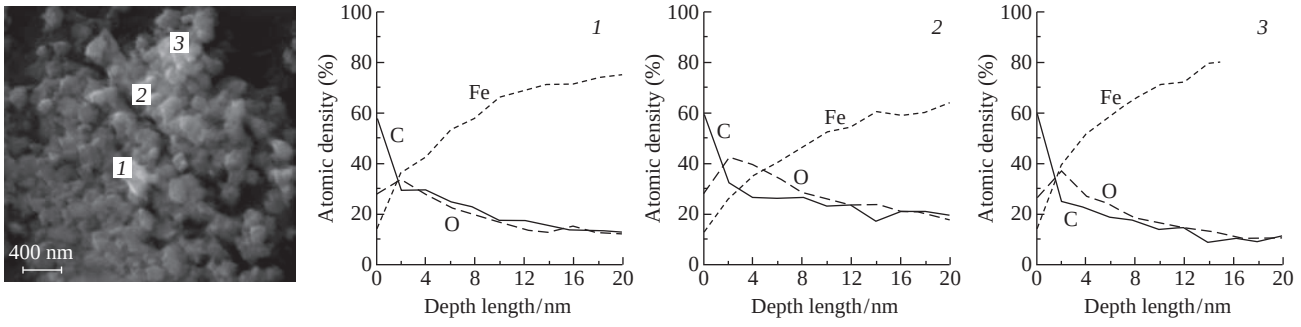

Figure 3 AES depth profiles of the near-surface composition of iron nanopowder after 20 min of passivation at three points obtained at room temperature.

References

1 E. O. Pentsak and V. P. Ananikov, *Mendeleev Commun*., 2014, **24**, 327.
2 A. B. Yaroslavtsev and Yu. P. Yampolskii, *Mendeleev Commun.*, 2014, **24**, 319.
3 M. V. Kuznetsov and G. S. Zakharova, *Mendeleev Commun.*, 2014, **24**, 17.
4 A. I. Gusev, A. S. Kurlov and A. A. Rempel, *Mendeleev Commun.*, 2015, **25**, 353.
5 M. N. Mayakova, A. A. Luginina, S. V. Kuznetsov, V. V. Voronov, R. P. Ermakov, A. E. Baranchikov, V. K. Ivanov, O. V. Karban and P. P. Fedorov, *Mendeleev Commun*., 2014, **24**, 360.
6 G. Brumfiel, *Nature*, 2003, **424**, 246.
7 M. H. A. Hassan, *Science*, 2005, **309**, 65.
8 W. Zhang, *J. Nanopart. Res*., 2003, **5**, 323.
9 O. Celebi, C. Üzüm, T. Shahwan and H. N. Erten, *J. Hazard. Mater*., 2007, **148**, 761.
10 S. M. Ponder, J. G. Darab and T. E. Mallouk, *Environ. Sci. Technol*., 2000, **34**, 2564.
11 F. Li, C. Vipulanandan and K. K. Mohanty, *Colloids Surf., A*, 2003, **223**, 103.
12 J. T. Nurmi, P. G. Tratnyek, V. Sarathy, D. R. Baer, J. E. Amonette, K. Pecher, C. Wang, J. C. Linehan, D. W. Matson, R. L. Penn and M. D. Driessen, *Environ. Sci. Technol*., 2005, **39**, 1221.
13 P. Varanasi, A. Fullana and S. Sidhu, *Chemosphere*, 2007, **66**, 1031.
14 M. O. Nutt, J. B. Hughes and M. S. Wong, *Environ. Sci. Technol*., 2005, **39**, 1346.
15 Y. Liu, S. A. Majetich, R. D. Tilton, D. S. Sholl and G. V. Lowry, *Environ. Sci. Technol*., 2005, **39**, 1338.
16 J. Cao, D. Elliott and W. Zhang, *J. Nanopart. Res*., 2005, **7**, 499.
17 J. Quinn, C. Geiger, C. Clausen, K. Brooks, C. Coon, S. O'Hara, T. Krug, D. Major, W.-S. Yoon, A. Gavaskar and T. Holdsworth, *Environ. Sci. Technol.*, 2005, **39**, 1309.
18 Y.-P. Sun, X. Li, J. Cao, W. Zhang and H. P. Wang, *Adv. Colloid Interface Sci*., 2006, **120**, 47.
19 L. Li, M. Fan, R. C. Brown, J. Van Leeuwen, J. Wang, W. Wang, Y. Song and P. Zhang, *Crit. Rev. Environ. Sci. Technol*., 2006, **36**, 405.
20 C. Noubactep, G. Meinrath, P. Dietrich, M. Sauter and B. J. Merkel, *Environ. Chem*., 2005, **2**, 71.
21 M. I. Alymov and O. N. Leontieva, *Nanostruct. Mater.*, 1995, **6**, 393.
22 R. Yuvakkumar, V. Elango, V. Rajendran and N. Kannan, *Dig. J. Nanomater. Biostruct*., 2011, **6**, 1771.
23 V. A. Zelensky, M. I. Alymov, A. B. Ankudinov and I. V. Tregubova, *Perspektivnye Materialy (Perspective Materials)*, 2009, no. 6, 83 (in Russian).
24 M. I. Alymov, N. M. Rubtsov, B. S. Seplyarskii, V. A. Zelensky and A. B. Ankudinov, *Mendeleev Commun.*, 2016, **26**, 452.
25 A. Rai, K. Park and M. R. Zachariah, *Combust. Theory Modell.*, 2006, **10**, 843.
26 O. Dufaud, A. Vignes, F. Henry, L. Perrin and J. Bouillard, *J. Phys.: Conf. Ser.*, 2011, **304**, 012076.
27 M. W. Beckstead, B. R. Newbold and C. A. Waroquet, in *50th JANNAF Propulsion Meeting*, CPIA Publication, 2001, vol. 1, pp. 201–220.
28 J. Bouillard, A. Vignes, O. Dufaud, L. Perrin and D. Thomas, *J. Hazard. Mater.*, 2010, **181**, 873.
29 C.-B.Wang and W.-X. Zhang, *Environ. Sci. Technol*., 1997, **31**, 2154.

Received: 18th April 2016; Com. 16/4911